

# Frictional behaviour of simulated muscovite fault gouge at shear strains up to 120 and temperatures of 20-600 °C

Esther van Diggelen, Christopher Spiers, Colin Peach & Gill Pennock

High Pressure and Temperature (HPT) laboratory, Faculty of Geosciences, PO Box 80.021, 3508 TA Utrecht, The Netherlands, Email: diggelen@geo.uu.nl



## 1. Introduction & problem

Phyllosilicates, such as muscovite, are common constituents of large-scale crustal fault zones and are widely expected to be relatively weak around the brittle-ductile transition, leading to low fault strength. However, quantitative data on the frictional strength of muscovite are limited, especially at large shear strains and under hydrothermal conditions.

The present study aims to investigate the frictional strength of phyllosilicates under hydrothermal conditions by determining the effects of temperature  $T$ , shear strain  $\gamma$ , sliding velocity  $V$  and effective normal stress  $\sigma_{eff}$ .

## 2. Action

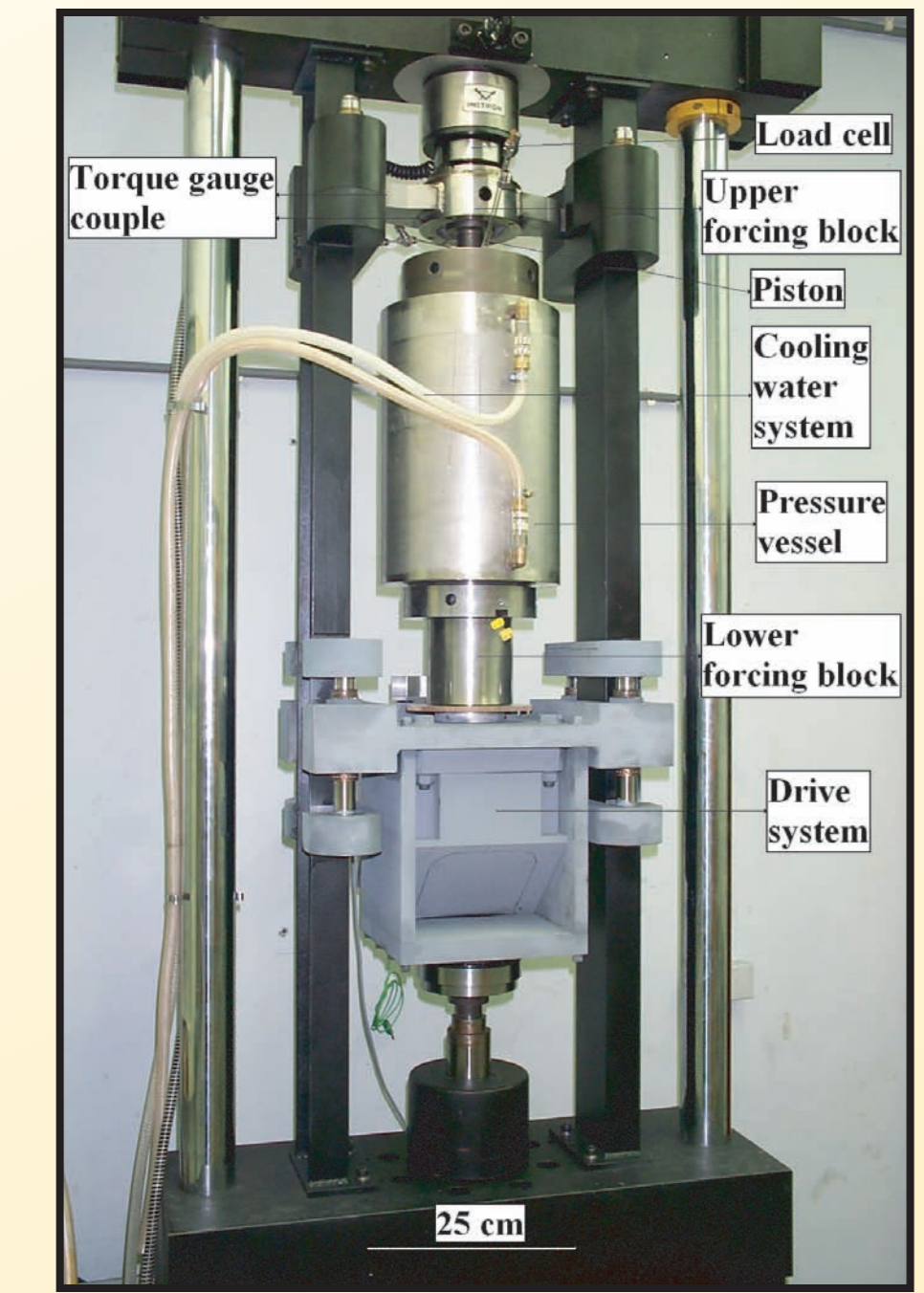


Figure 1: Experimental set up.

### Rotary shear experiments:

- Normal stress-stepping experiments
- Velocity-stepping experiments
- Experiments at constant  $V$  and  $\sigma_{eff}$

### Materials:

Sample: Muscovite gouge  
average grainsize  $d=13 \mu\text{m}$   
~10% quartz impurities  
Pore fluid: Deionised water

### Conditions:

- Fluid pressure  $P_f$ : 100 MPa
- Temperature  $T$ : 20-600°C
- Effective normal stress  $\sigma_{eff}$ : 20-100 MPa
- Sliding velocity  $V$ : 0.03-3.8  $\mu\text{m/s}$
- Shear strain  $\gamma$ : up to 120
- Shear strain rates:  $\sim 10^{-3}$ - $10^{-5} \text{ s}^{-1}$

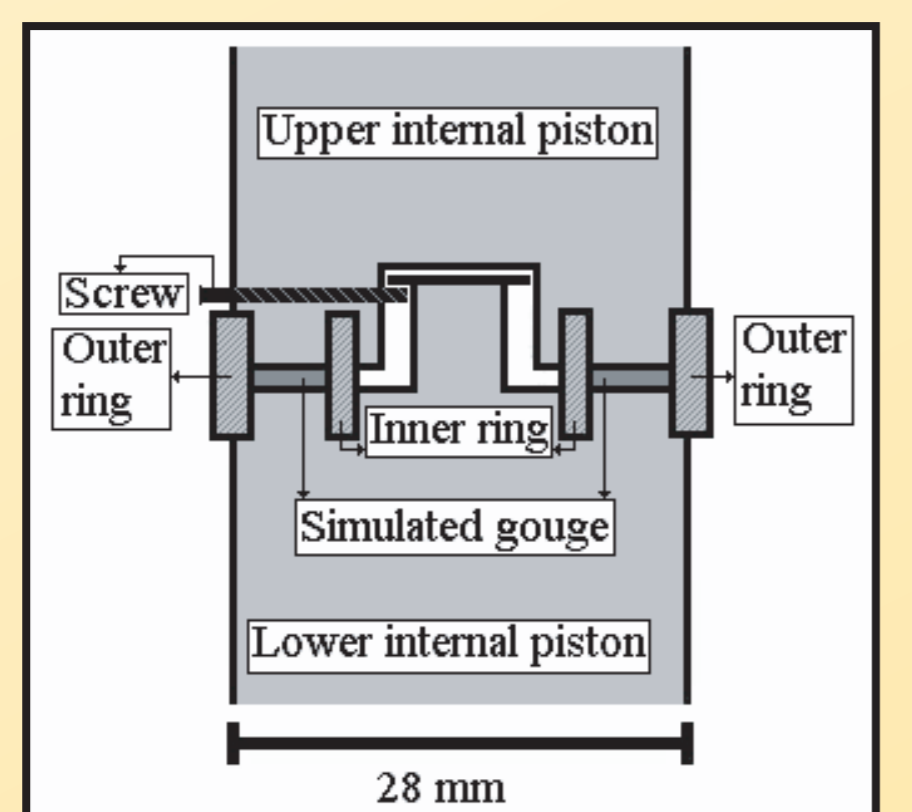


Figure 2: Schematic diagram of the experimental set up.

## 3. Mechanical behaviour

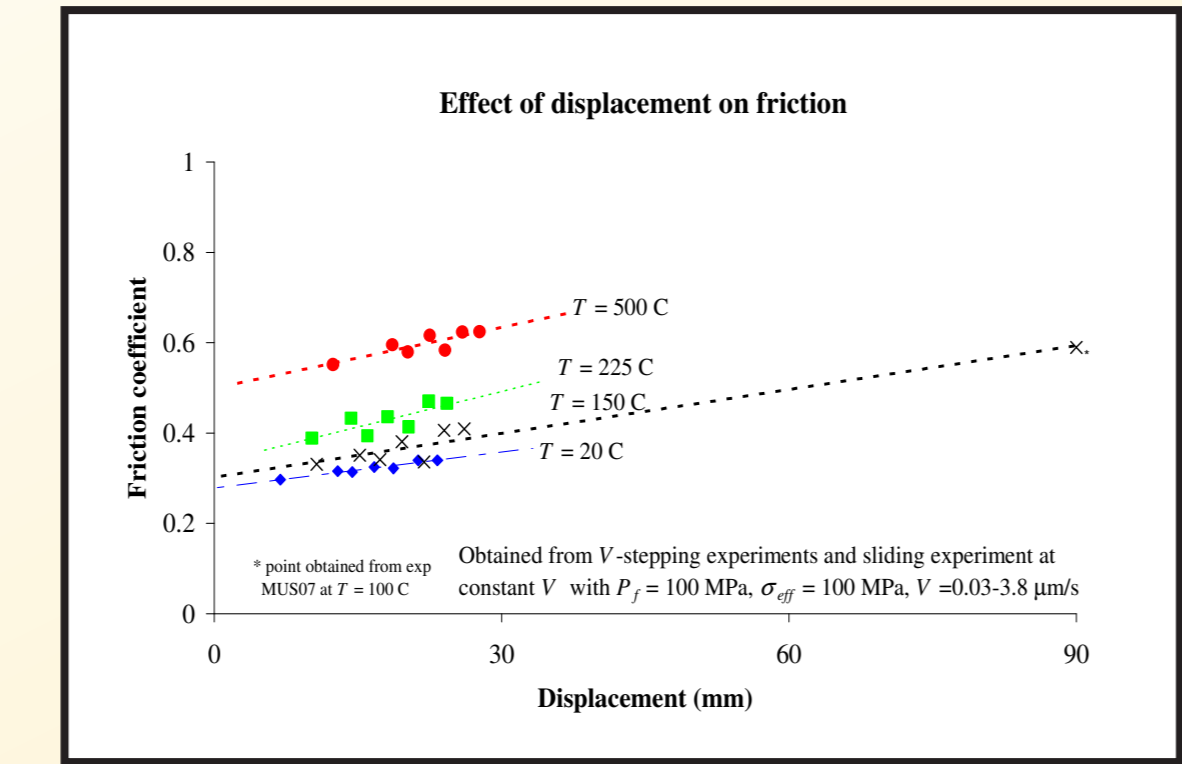


Figure 3: Friction coefficient  $\mu$  versus displacement. Temperature as indicated.

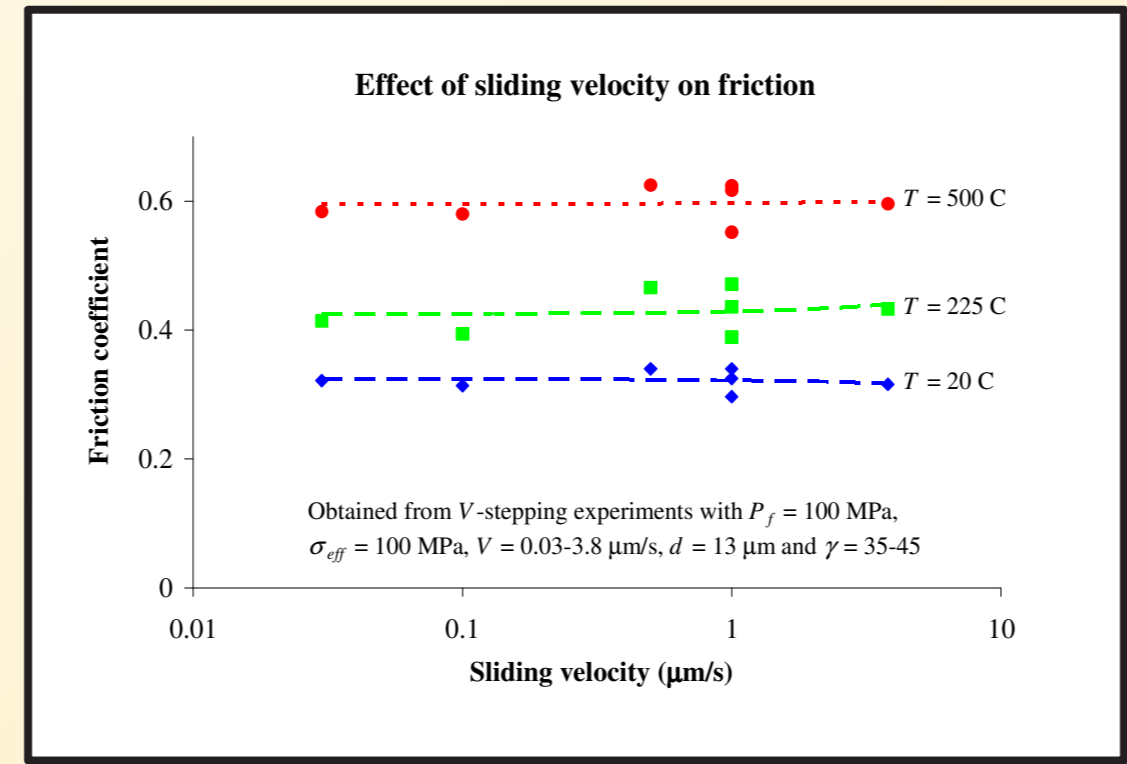


Figure 4: Friction coefficient versus log sliding velocity. Temperature as indicated.

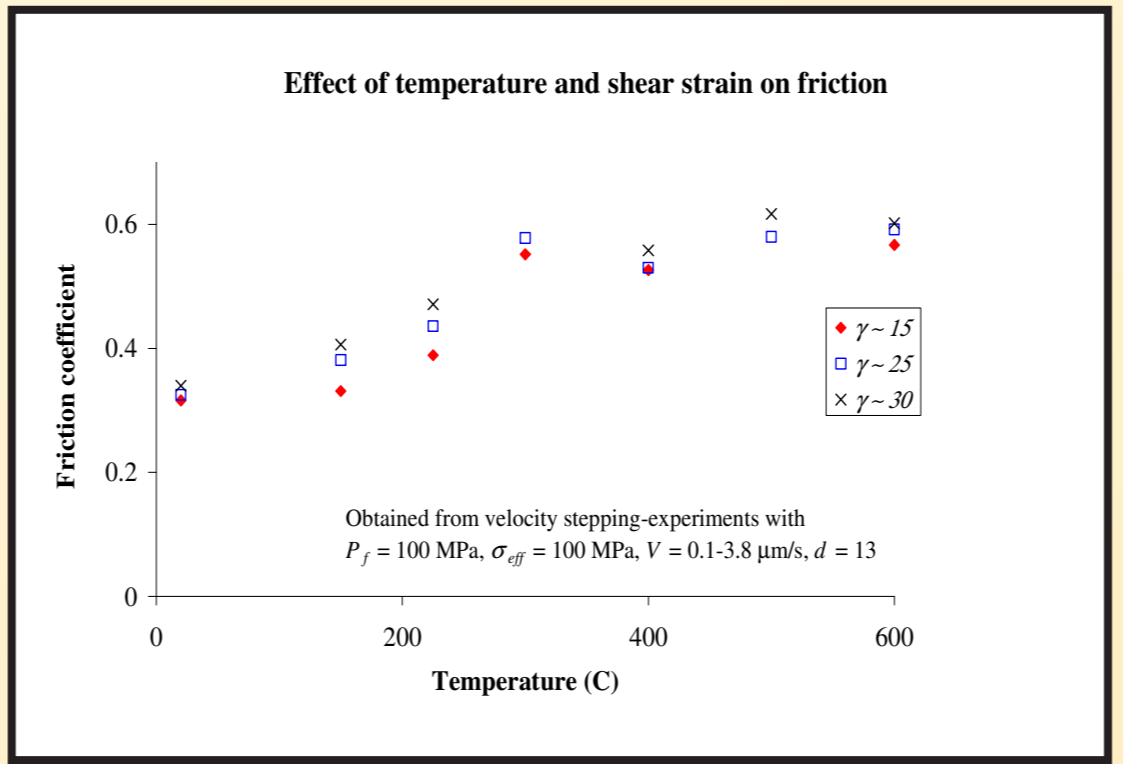


Figure 5: Friction coefficient versus temperature. Shear strain as indicated.

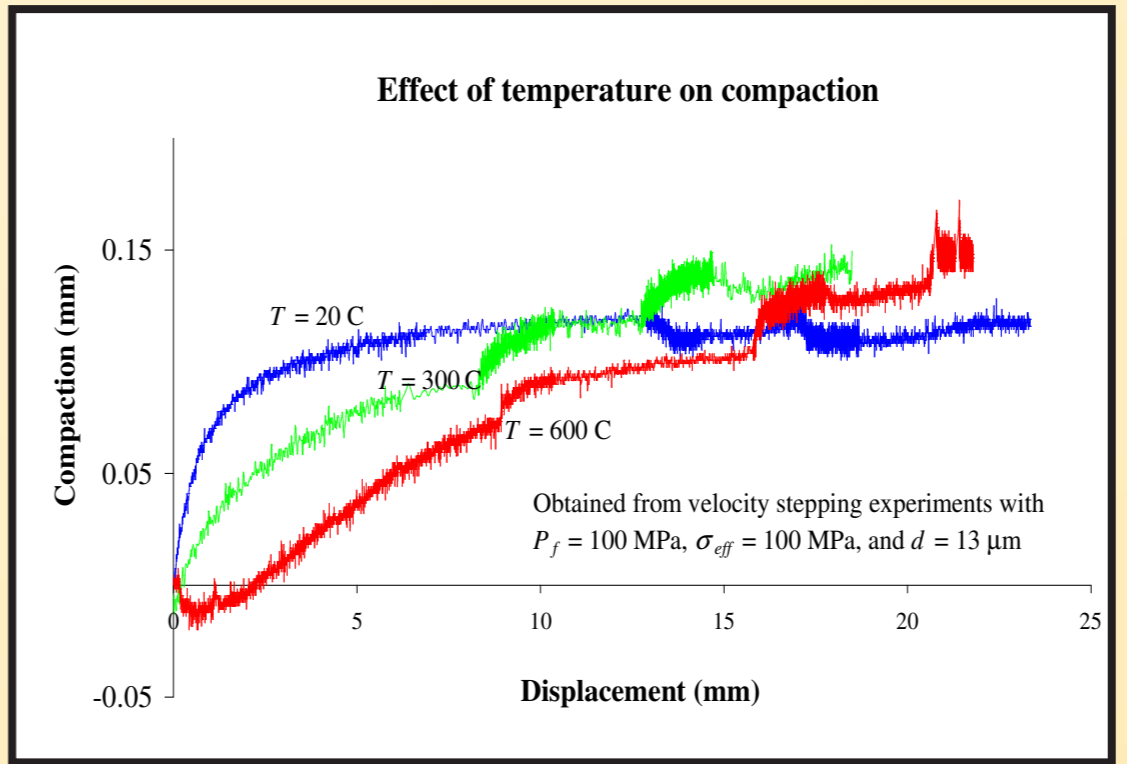


Figure 6: Compaction versus displacement. Temperature as indicated.

- Friction coefficient  $\mu$  increases with displacement ( $\gamma$ ) at all  $T$ .
- $\mu$  independent of  $V$  at all  $T$ .
- $\mu$  increases with  $T$ , notably from 200-300 °C.
- $\mu$  remains constant in the range 300-600 °C.
- Compaction increases with  $\gamma$ .
- At  $\gamma < 15$  compaction decreases with  $T$ .
- Dilatation at low  $\gamma$  at  $T > 300^\circ\text{C}$ .

## 4. Microstructures and deformation mechanisms

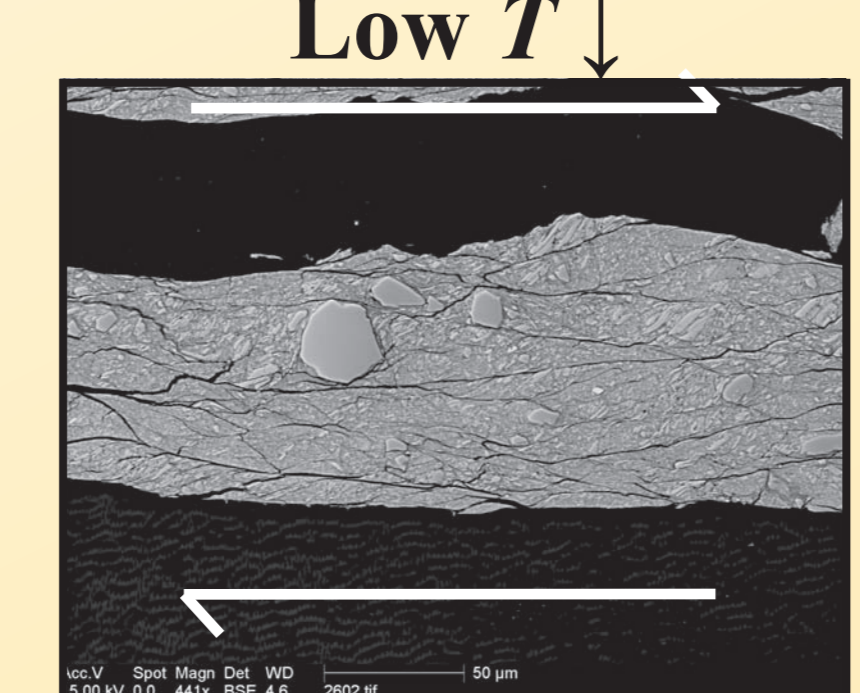


Figure 7: MUS26,  $T=150^\circ\text{C}$ ,  $\gamma=35$ ,  $\sigma_{eff}=100 \text{ MPa}$ ,  $V=0.03\text{-}3.8 \mu\text{m/s}$ .

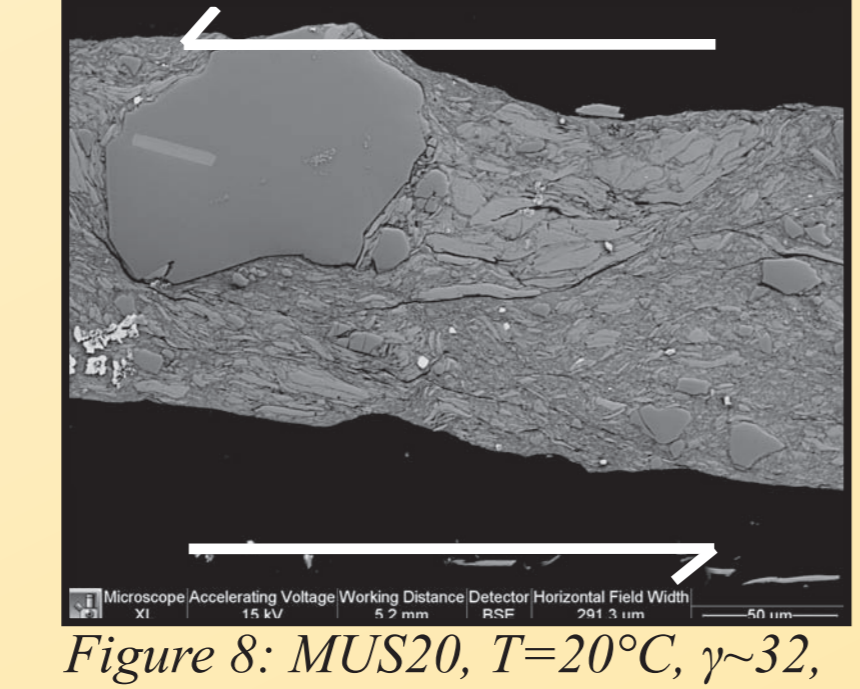


Figure 8: MUS20,  $T=20^\circ\text{C}$ ,  $\gamma=32$ ,  $\sigma_{eff}=100 \text{ MPa}$ ,  $V=0.03\text{-}3.8 \mu\text{m/s}$ .

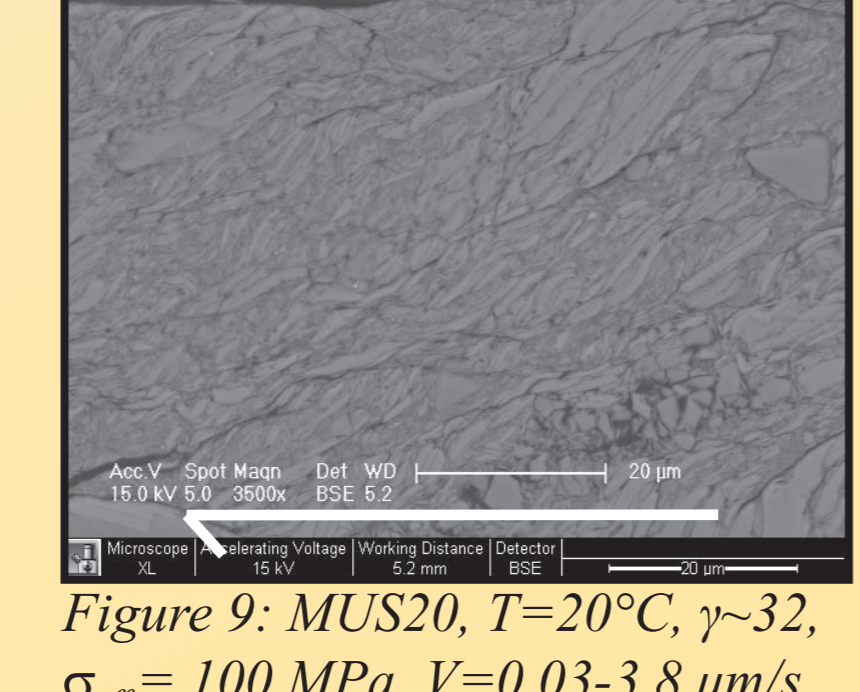


Figure 9: MUS20,  $T=20^\circ\text{C}$ ,  $\gamma=32$ ,  $\sigma_{eff}=100 \text{ MPa}$ ,  $V=0.03\text{-}3.8 \mu\text{m/s}$ .

- ### Low T (20-225 °C)
- Strong grainsize reduction to form a well foliated matrix ( $< 2 \mu\text{m}$ ).
  - Widespread quartz and muscovite porphyroclasts ( $\sim 10 \mu\text{m}$ ).
  - Structure cross cut by shear bands in Riedel and Y-shear orientations.

- ### High T (300-600 °C)
- Increasingly characterised by dense, elongate lenses ( $30 \times 10 \mu\text{m}$ ), separated by an anastomosing network of ultra-fine ( $< 1 \mu\text{m}$ ) cataclastic zones.
  - Lenses consist of fine, folded and kinked grains ( $5\text{-}10 \mu\text{m}$ ).

Deformation mechanisms	
Low T	High T
1. Cataclastic flow 2. Particle alignment/slip giving a foliation	1. Cataclastic flow 2. Plastic deformation/kinking 3. Healing by diffusive mass transfer processes

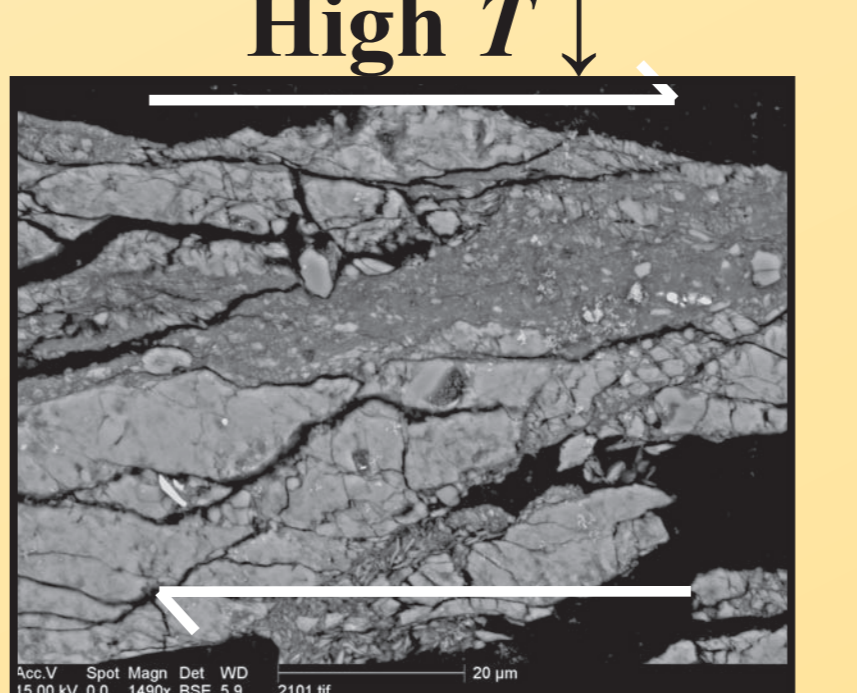


Figure 10: MUS21,  $T=500^\circ\text{C}$ ,  $\gamma=85$ ,  $\sigma_{eff}=100 \text{ MPa}$ ,  $V=1.0 \mu\text{m/s}$ .

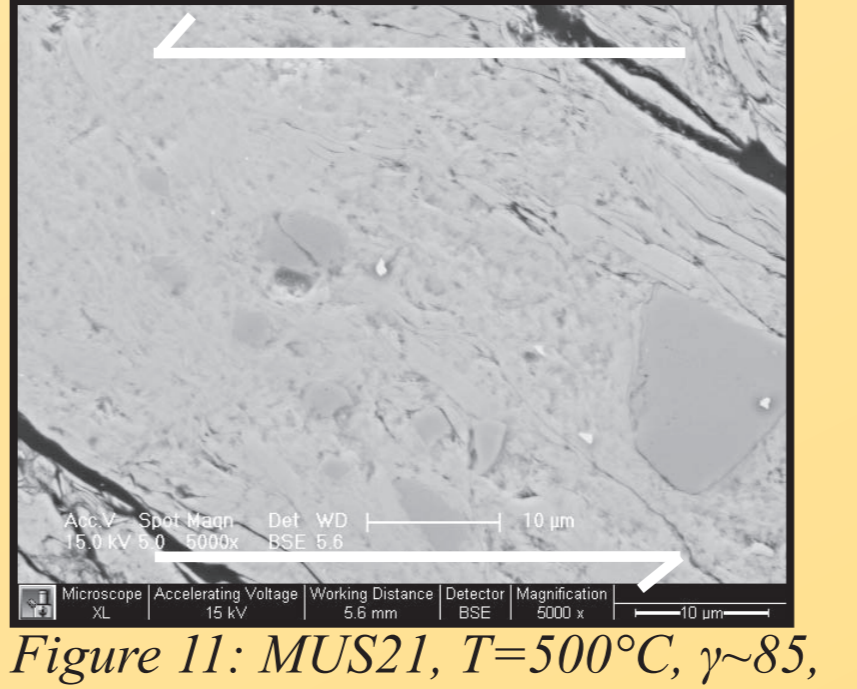


Figure 11: MUS21,  $T=500^\circ\text{C}$ ,  $\gamma=85$ ,  $\sigma_{eff}=100 \text{ MPa}$ ,  $V=1.0 \mu\text{m/s}$ .

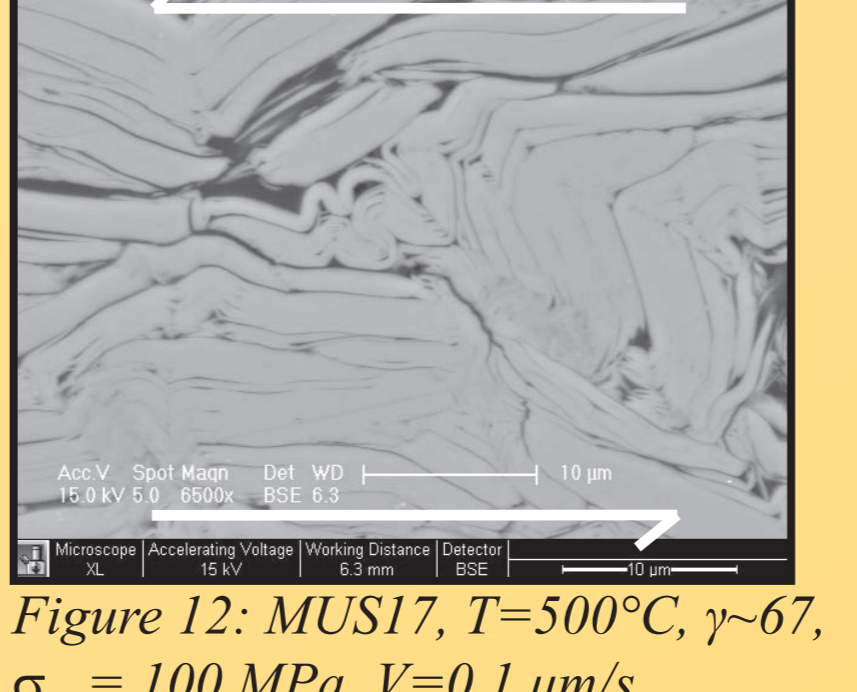
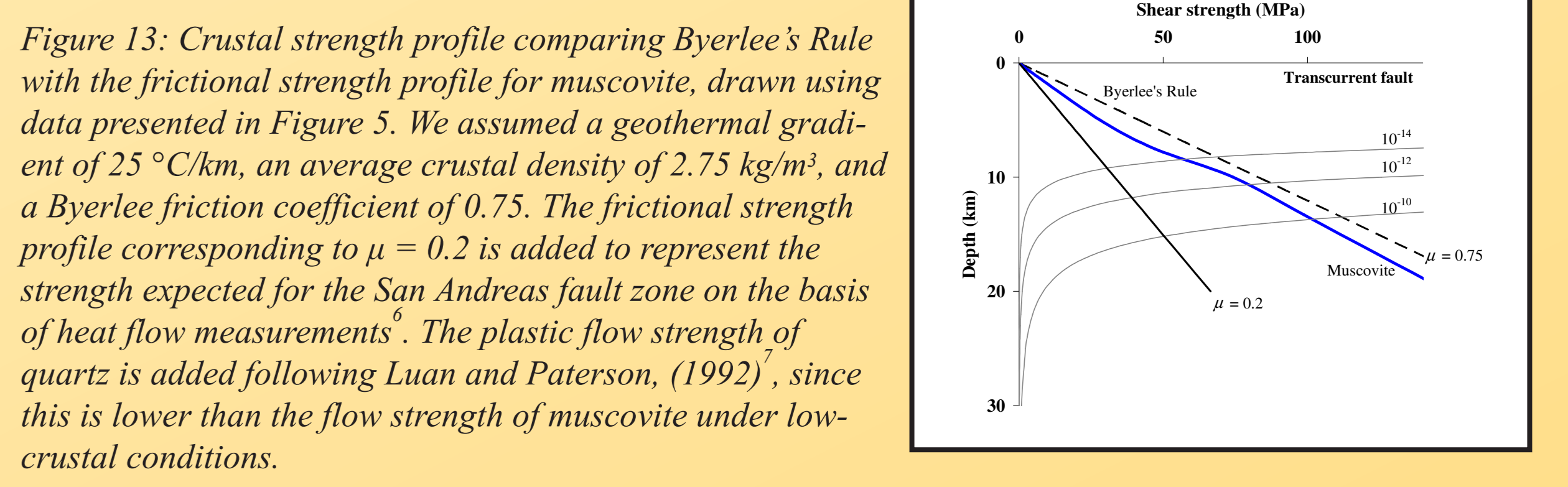


Figure 12: MUS17,  $T=500^\circ\text{C}$ ,  $\gamma=67$ ,  $\sigma_{eff}=100 \text{ MPa}$ ,  $V=0.1 \mu\text{m/s}$ .

## 5. Discussion & conclusions

- The friction coefficient of muscovite increases from  $\sim 0.33$  to  $\sim 0.44$  in the temperature range 20-225 °C, reaching 0.57 at  $T=300\text{-}600 \text{ }^\circ\text{C}$ .
- The low  $T$  friction coefficient is in agreement with values previously reported in the literature<sup>1-4</sup>. However, the high  $T$  value is higher than previously reported<sup>5</sup>, possibly due to the strain hardening effects seen in our high strain experiments.
- No rate-depedent behaviour (e.g. dislocation/diffusion creep) was observed even at the highest temperature studied. Such effects have been previously reported<sup>5</sup> at  $T=700 \text{ }^\circ\text{C}$ , and at strain rates below  $10^{-5} \text{ s}^{-1}$ .



- In the frictional regime, muscovite fault gouge is, even after strain hardening, weaker than most rocks that obey Byerlee's Rule ( $\mu = 0.60\text{-}0.85$ ), but only slightly (Figure 13).
- The frictional strength of muscovite gouge is not low enough to explain the weakness inferred for faults, such as the San Andreas fault zone, from geological and geophysical evidence<sup>6</sup>.
- Next step: Determine the behaviour of quartz / muscovite mixtures under hydrothermal conditions.

### References:

- 1) Scruggs V.J. & T.E. Tullis (1998), Tectonophysics, 295, 15-40.
- 2) Moore D.E. & D.A. Lockner (2004), JGR, 109, doi: 10.1029/2003JB002582.
- 3) Morrow C.A., et al. (2000), GRL, 27, 815-818.
- 4) Mares V.M. & A.K. Kronenberg (1993), JSG, 15, 1061-1075.
- 5) Mariani E. et al. (2006), JSG, 28, 1-19.
- 6) Lachenbruch, A.H. & J. H. Sass (1980), JGR, 85, 6185-6222.
- 7) Luan, F.C. & M.S. Paterson (1992), JGR, 97, 301-320.

Acknowledgements: We thank Thony van der Gon, Gert Kastelein, Peter van Krieken and Eimert de Graaff for technical support. This study was funded by the Netherlands Research Centre for Integrated Solid Earth Science (ISES).